IconShop: Text-Guided Vector Icon Synthesis with Autoregressive Transformers

RONGHUAN WU, City University of Hong Kong
WANCHAO SU, City University of Hong Kong
KEDE MA, City University of Hong Kong
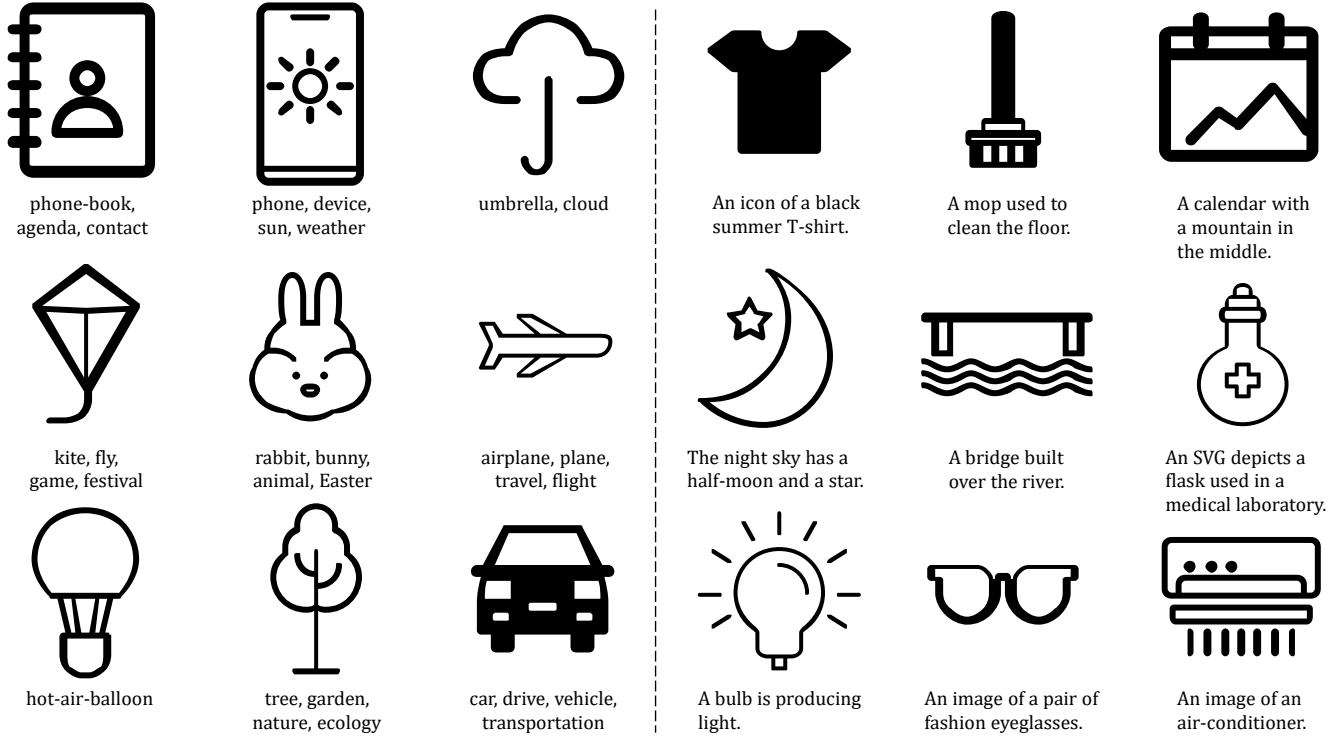JING LIAO*, City University of Hong Kong

Fig. 1. Vector icons generated with text prompts. The proposed IconShop supports vector icon synthesis from keywords (left panel) and natural phrases and sentences (right panel).

Scalable Vector Graphics (SVG) is a popular vector image format that offers good support for interactivity and animation. Despite its appealing characteristics, creating custom SVG content can be challenging for users due to the steep learning curve required to understand SVG grammars or get familiar with professional editing software. Recent advancements in text-to-image generation have inspired researchers to explore vector graphics synthesis using either image-based methods (i.e., text → raster image → vector graphics) combining text-to-image generation models with image vectorization, or language-based methods (i.e., text → vector graphics script) through pretrained large language models. However, these methods still suffer from limitations in terms of generation quality, diversity, and flexibility. In this paper, we introduce IconShop, a text-guided vector icon synthesis method using autoregressive transformers. The key to success of our approach is to sequentialize and tokenize SVG paths (and textual descriptions as guidance) into a uniquely decodable token sequence. With that, we are able to fully exploit the sequence learning power of autoregressive transformers, while enabling both unconditional and text-conditioned icon synthesis. Through standard training to predict the next token on a large-scale vector icon dataset accompanied by textural descriptions, the proposed IconShop consistently exhibits better icon synthesis capability than existing image-based and language-based methods both quantitatively (using the FID and CLIP scores) and qualitatively (through formal subjective user studies). Meanwhile, we observe a dramatic improvement in generation diversity, which is validated by the objective Uniqueness and Novelty measures. More importantly, we demonstrate the flexibility of IconShop with multiple novel icon synthesis tasks, including icon editing, icon interpolation, icon semantic combination, and icon design auto-suggestion. The project page is https://icon-shop.github.io/.

*Corresponding Author.
Authors' addresses: Ronghuan Wu, City University of Hong Kong, ronghwu2-c@my.cityu.edu.hk; Wanchao Su, City University of Hong Kong, wanchao_su@outlook.com; Kede Ma, City University of Hong Kong, kede.ma@cityu.edu.hk; Jing Liao*, City University of Hong Kong, jingliao@cityu.edu.hk.

Additional Key Words and Phrases: SVG, Icon Generation, Vector Graphics Synthesis, Text-Guided Generation, Autoregressive Transformers.

1 INTRODUCTION

As a form of computer graphics, vector graphics represents visual content based directly on geometric shapes (via command lines and arguments) and is widely used in scientific and artistic applications, including architecture, surveying, 3D rendering, typography, and graphic design. Compared with raster images, vector graphics is preferred when a high degree of geometric precision is required across arbitrary scales. Scalable Vector Graphics (SVG) is a popular vector graphics file format, particularly in creative industries. However, creating SVG content is generally difficult for non-professional users. It is tedious and time-consuming to gain adequate knowledge of SVG grammars and/or master professional editing software such as Adobe Illustrator. Recently, there have been impressive successes in generating raster images from text, providing a convenient and efficient means of generating high-quality images that fulfill users' design intents. Thus, it is highly desirable to build a computational system that can accomplish something similar in the field of SVG, allowing for accurate and flexible SVG content synthesis guided by intuitive textual descriptions.

One straightforward approach is adapting image generation to vector synthesis by converting the image outputs of text-to-image generation models into vector graphics using image vectorization methods. While such image-based methods (i.e., text → raster image → vector graphics) directly incorporate recent advances in text-to-image generation (e.g., Stable Diffusion [Rombach et al. 2022]) into SVG generation, their results are often unsatisfactory. This is because text-to-image generation models are trained on raster images, which tend to produce complex images that are difficult to resemble SVG styles with simple geometric primitives and flat colors. Furthermore, to accommodate these complex images, vectorization methods often use unsmooth paths with sharp corners and crossovers, resulting in artifacts in the final SVG results.

As SVG is based on Extensible Markup Language (XML), one research avenue for synthesizing SVG content is to train Sequence-To-Sequence (seq2seq) language models that take text prompts as input and directly produce SVG scripts as output. This kind of method is referred to as language-based (i.e., text → vector graphics script) approaches. Despite its conceptual simplicity, SVG involves complex grammars. Naive tokenization of text as natural language for SVG can result in complex and lengthy token sequences, complicating subsequent probabilistic modeling. Preliminary experiments [Bubeck et al. 2023] show that Large Language Models (LLMs) like GPT-4 [OpenAI 2023] can combine basic geometric shapes, such as `Circle` and `Ellipse`, to convey semantic information with relatively good text-SVG alignment. However, the results show limited complexity and diversity in generation (see Section 4.3), which is inadequate for real-world SVG applications.

In this paper, we develop an autoregressive transformer-based method that supports accurate and flexible SVG content synthesis guided by textual descriptions. We demonstrate the feasibility of our method in the context of SVG icons, giving rise to the name, IconShop. The key to success of IconShop is to exploit the sequential

nature of SVG: An SVG script is composed of a sequence of paths, which in turn consists of a sequence of drawing commands (e.g., lines and curves, see Section 3.2). We thus concatenate all SVG paths in a uniquely decodable way to form a command sequence. Since the text prompt is sequential in nature as well, it can be straight-forwardly prepended to the command sequence. We thus tokenize and mask the combined sequence in a way [Aghajanyan et al. 2022; Bavarian et al. 2022; Fried et al. 2023] that IconShop admits standard training (to predict the next token autoregressively) and enables conditional SVG icon synthesis on the bidirectional context (i.e., the fill-in-the-middle task). This can be effectively achieved by incorporating the right context into the left context (separated by a special token), which conforms to causal (i.e., autoregressive) masking.

We train IconShop on a large-scale vector icon dataset *FIGR-8-SVG* [Clouâtre and Demers 2019], consisting of monochromatic (i.e., black-and-white) SVG icons. We conduct comprehensive evaluations of IconShop in terms of generation quality and diversity under different synthesis settings. Our experimental results show that IconShop is superior to existing image-based and language-based methods in these two aspects both quantitatively and qualitatively. The synthesized SVG icons also show reasonable faithfulness to the corresponding text prompts. Moreover, we demonstrate the flexibility of IconShop with multiple novel icon synthesis tasks, including icon editing, icon interpolation, icon semantic combination, and icon design auto-suggestion.

2 RELATED WORK

Our work is related to text-to-image generation (Section 2.1), vector graphics generation (Section 2.2) and generative transformers (Section 2.3). Here we only provide a concise review of previous work that is closely related to ours, and a comprehensive treatment of the above areas is beyond the scope of this paper.

2.1 Text-to-Image Generation

Generating images from text is a challenging task that has gained substantial attention in recent years and has gone through three stages of development: Generative Adversarial Networks (GANs) [Kang et al. 2023; Qiao et al. 2019; Reed et al. 2016; Xu et al. 2018; Zhang et al. 2017, 2018], seq2seq models based on transformers [Chang et al. 2023; Ding et al. 2021, 2022; Ramesh et al. 2021; Yu et al. 2022], and diffusion models [Nichol et al. 2021; Rombach et al. 2022; Saharia et al. 2022]. Specifically, a GAN [Goodfellow et al. 2014] involves training two neural networks - a generator and a discriminator - to play a minmax zero-sum game. The system learns to generate new images by respecting the training data distribution and text conditions. However, text-conditioned GANs [Kang et al. 2023; Qiao et al. 2019; Reed et al. 2016; Xu et al. 2018; Zhang et al. 2017, 2018] are typically limited to modeling single and multiple object classes. Scaling them up to handle complex image datasets remains very challenging due to the instability occurred in the training procedure, until very recently Kang et al. [2023]. Seq2seq models based on transformers operate by converting (and concatenating) the input text (and image) into a sequence of tokens for predicting another sequence of tokens that corresponds to the target image [Chang et al. 2023; Ding et al. 2021, 2022; Ramesh et al. 2021; Yu et al. 2022]. Text-only

and image-only self-attention and text-image cross-attention are canonical computational mechanisms in seq2seq models to capture intricate dependencies between text and image tokens. Recently, diffusion models have emerged to be the new standard in text-to-image generation overnight. Typically, an unconditional diffusion model [Ho et al. 2020] initiates its process with Gaussian noise, and iteratively eliminates it to yield a natural image. Text-guided diffusion models [Nichol et al. 2021; Rombach et al. 2022; Saharia et al. 2022] leverage the text embedding either as input or through cross-attention. Although previous work tackles text-guided visual content generation like ours, they focus primarily on raster images with fixed resolution. In contrast, we aim for a different goal - text-guided vector icon synthesis with arbitrary scaling.

2.2 Vector Graphics Generation

In the early 2000s, SVG content can be created using PERL [Probets et al. 2001] with plentiful drawing commands, but requires extensive human intervention. Bergen and Ross [2012] automates the determination of the number and type of drawing commands by evolutionary computation to match a target raster image. These work can be seen as seeding works in vector graphics generation. Recent attempts toward vector content generation gain significant progress with deep neural networks by learning useful SVG representations for editing and manipulation. SketchRNN [Ha and Eck 2017] is a pioneering deep representation learning model for vector sketches based on a seq2seq Variational Auto-Encoder (VAE) [Kingma and Welling 2013]. The encoder and the decoder were implemented by a bidirecrtional recurrent neural network (RNN) and an autoregressive RNN, respectively. The sketches are parameterized by polylines - a sequence of points with line segments drawn between consecutive points. Lopes et al. [2019] incorporate a VAE-learned raster image representation to aid SVG font synthesis. The feasibility of the method is demonstrated only on glyphs with a maximum of 50 commands. Modeling the hierarchical structure of SVG, DeepSVG [Carlier et al. 2020] trains two transformer-based encoders in tandem to transform SVG icons from commands to path-level representations, and then to a global latent representation. Two decoders are paired up for SVG icon reconstruction. Although the reconstructed shapes look generally reasonable, DeepSVG fails to reproduce geometric relationships like perpendicularity and parallelism. Inspired by DeepSVG, Aoki and Aizawa [2022] make full use of the global latent representation in every stage of the decoder for synthesizing Chinese SVG characters. Despite the success of the above-mentioned methods, they fail to support text-guided generation.

To enable synthesizing SVG contents with text input, recent methods usually resort to pretrained vision-language models. One straightforward approach is to first generate a raster image with a pretrained text-to-image generation model (e.g. DALL·E [Ramesh et al. 2021], Stable Diffusion [Rombach et al. 2022]), then vectorize it using some image vectorization techniques (e.g. Potrace [Selinger 2003], LIVE [Ma et al. 2022]). Another line of work that has emerged recently is directly optimizing SVG parameters with the guidance of pretrained vision-language models. For instance, CLIPDraw [Frans et al. 2021] achieves text-to-vector drawing synthesis by comparing the rasterized image version of the vector result (with DiffVG [Li

et al. 2020]) in the CLIP [Radford et al. 2021] space to calculate its distance to the input textual description during generation. Instead of using CLIP distance, VectorFusion [Jain et al. 2022] distills abstract semantic knowledge from a pretrained diffusion model. It first vectorizes a text-to-image diffusion sample with LIVE [Ma et al. 2022] and then fine-tunes SVG parameters with a Score Distillation Sampling (SDS) loss [Poole et al. 2022] on pretrained Stable Diffusion [Rombach et al. 2022]. However, both modalities share same limitations in SVG generation: First, as these vision-language models are pretrained on raster images, it is challenging for them to provide guidance in generating SVG-style images with simple geometric primitives and flat colors, often leading to complex vector graphics. Second, whether directly optimizing path parameters from losses defined by vision-language models or vectorizing generated images, the resulting paths are often jagged and messy, failing to reproduce accurate geometric relations such as parallelism and perpendicularity. Third, the per-SVG optimization can be painfully slow, making it impractical for real-time applications. In contrast, our proposed system, IconShop, does not suffer from any of the above-mentioned problems. As our model directly generates command sequences, it can guarantee simplicity and regularity in synthesized SVG results. Moreover, once trained, IconShop can perform text-guided vector icon synthesis automatically and efficiently.

2.3 Transformers as Generative Models

Owing to its inherent capability to capture long-term dependencies and support parallel computing, Transformers [Vaswani et al. 2017] have emerged as a powerful class of generative models for producing a wide range of outputs, ranging from natural languages [Brown et al. 2020; Radford et al. 2019; Raffel et al. 2020], audios [Huang et al. 2018; Li et al. 2019; Valle et al. 2020], and raster images [Chen et al. 2020; Esser et al. 2021]. Transformers can be made non-autoregressive and autoregressive. The non-autoregressive instantiation [Chang et al. 2023, 2022; Ding et al. 2022; Zhang et al. 2021] suggests to leverage the bidirectional context using BERT-like [Devlin et al. 2018] bidirectional Transformers for its sampling efficiency and adaptation ability to different image manipulation tasks. The autoregressive instantiation [Ding et al. 2021; Ramesh et al. 2021; Yu et al. 2022] emphasizes the importance of learning to predict the next token in a causal way. Together with scaling, it unlocks the emerging abilities in LLMs. Inspired by [Aghajanyan et al. 2022; Bavarian et al. 2022], here we unify non-autoregressive and autoregressive modeling of vector icons for various synthesis tasks.

3 ICONSHOP

In this section, we first briefly introduce autoregressive models (Section 3.1) and then describe the SVG commands of vector icons and our tokenization strategy (Section 3.2). We also describe our "causal" masking strategy, which enables our autoregressive model to fill in missing information by leveraging bidirectional contexts (Section 3.3). We next elaborate our model architecture (Section 3.4) and, finally, present the training objectives (Section 3.5).
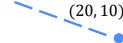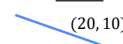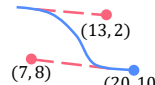
Name	Symbol	Argument	Explanation	Example
Move To	M	x, y	Move the cursor to the specified point (x, y).	
Line To	L	x, y	Draw a line segment from the current point to the specified point (x, y).	
Cubic Bézier	C	x_1, y_1 x_2, y_2 x, y	Draw a curved path from the current point to the specified point (x, y) using two control points (x_1, y_1) and (x_2, y_2).	

Table 1. Overview of SVG commands. In our implementation, we employ three simple yet expressive commands (namely, M, L, and C) to represent vector icons. In the Example column, we assume the current point is located at $(0, 0)$. For a sequence of commands, the starting position of each command is the ending position of the previous command.

3.1 Preliminaries on Autoregressive Models

An autoregressive model specifies that the current state depends only on its previous states. In probabilistic terms, this corresponds to the chain rule of probability:

$$p(s) = \prod_{n=1}^{N} p(s_n | s_1, \ldots, s_{n-1}), \tag{1}$$

in which we factorize the joint probability of a sequence of random variables $s = (s_1, \ldots, s_N)$ into a product of conditional probabilities. At the n-th instance, autoregressive models take the values of previous $n - 1$ random variables (or the most recent ones if a Markov window is applied) as input, and compute the conditional probability distribution of s_n, from which we are able to draw a sample as its prediction. Here we resort to autoregressive models for SVG icon synthesis because it fits naturally in the sequential nature of SVG as well as textural descriptions as guidance.

3.2 SVG Representation and Tokenization

SVG offers a range of features and syntax options, allowing users to present their creative works with greater flexibility. For example, the Rect command creates a rectangular shape controlled by the starting point, width, and height arguments, like <Rect x="80" y="90" width="100" height="100"/>. The Transform attribute applies an affine transformation to an existing shape element instead of creating a new one, like <Rect Transform="rotate (-10 50 100)" x="80" y="90" width="100" height="100"/>. However, if we develop a data structure for each command and attribute and incorporate them into the training process, the input data would become highly complex. This complexity would increase the difficulties in training the model, resulting in unsatisfactory quality. To address this issue, we need to limit the number of commands and attributes to maintain the model's performance. The selected commands and attributes should be capable of accurately capturing the essential information in an SVG icon. In simpler terms, we require a straightforward and concise representation that conveys the critical aspects of the SVG icon.

Inspired by DeepSVG [Carlier et al. 2020], we simplify every SVG icon by removing all attributes and using only three basic commands:

Move To, Line To, and Cubic Bézier (see Table 1 for explanations and examples) to represent SVG icons. Other complex commands (e.g., Rect, Circle, Ellipse, etc.) can be approximated by combinations of these basic commands without sacrificing details. For example, we can use four line segments to construct a Rect, and concatenate four Bézier curves to form a Circle. An SVG text script V contains multiple *paths*, $V = \{P_1, \ldots, P_{N_P}\}$, where P_i is the i-th path and N_P is the number of paths. Each path P_i in turn consists a sequence of *commands*, $P_i = (C_i^1, \ldots, C_i^{N_{C_i}})$, where C_i^j is the j-th command and N_{C_i} is the total number of commands for path i. A command, $C_i^j = (c_i^j, X_i^j)$, contains its type $c_i^j \in \{M, L, C\}$ and corresponding 2D parameter X_i^j.

After simplifying the SVG icons as described above, they are now in a uniform representation. The next step is to convert the SVG text scripts into discrete sequences of tokens for an AR model to predict. We present an intuitive and efficient tokenization approach for SVG text scripts. This method includes the following four steps: 1) Flatten the hierarchical structures of the SVG by concatenating commands of different paths to form a single sequence that contains all commands of an SVG. To make this process reversible (i.e., breaking down the sequence back into its original individual paths), we prepend a special token, <BOP> (i.e., *begin-of-path*), before the first command of each path; 2) Assigning distinct numbers to each command type (i.e., M, L, C); 3) Converting 2D coordinates into 1D format. Suppose the width of an SVG image is w, we transform a 2D point $X = (x_0, y_0)$ to a 1D coordinate using the formula $x_0 \times w + y_0$. This halves the length of argument token sequences, allowing us to process more data within the same length limit; 4) Append a special token, <EOS> (i.e., *end-of-SVG*), at the end of the sequence that indicates the completion of an SVG icon sequence. An example of a sequence created using the above steps is shown in Figure 2.

3.3 Masking Scheme

Autoregressive models have been shown to be effective in generating token sequences from scratch in previous works, but they are limited to generating tokens in a single direction (i.e., from left to right). This restriction hinders performance in tasks such as icon editing, where we need to fill in missing content based on bidirectional
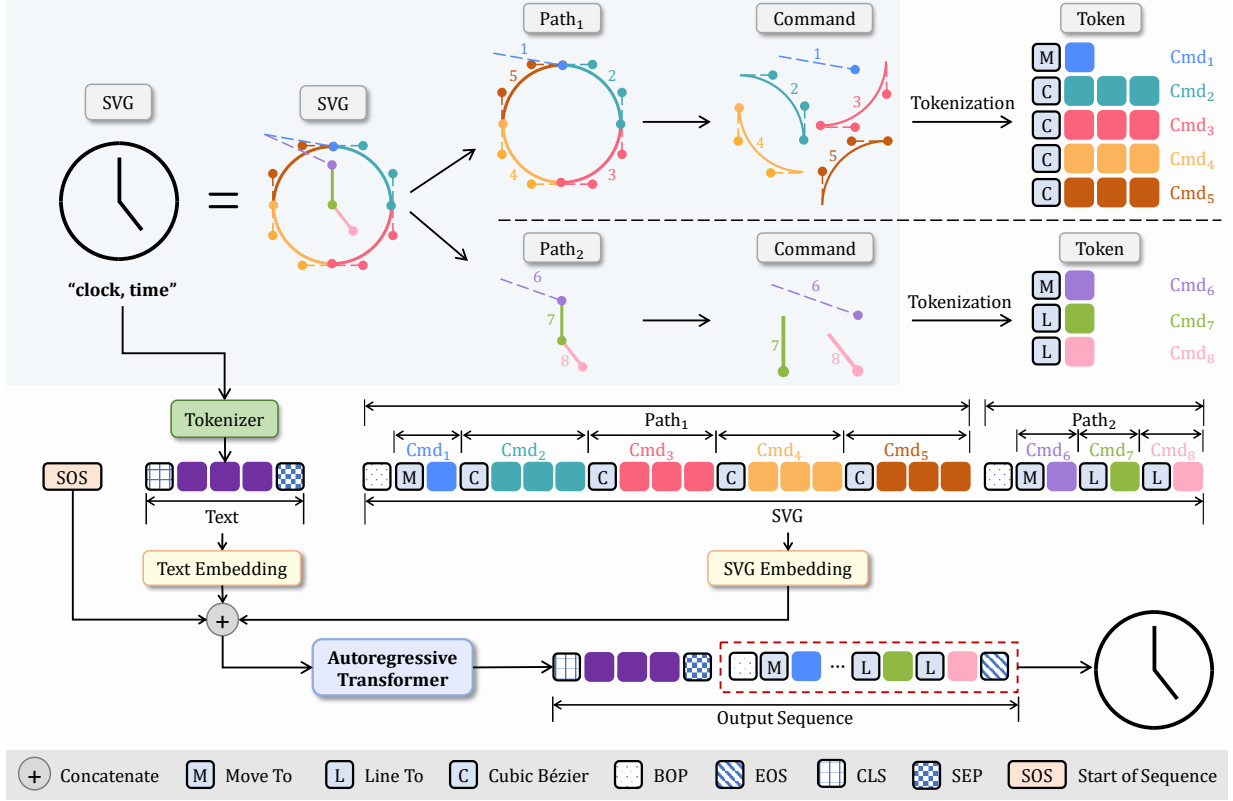
Fig. 2. The pipeline of IconShop. In this example, the clock **icon** has two paths, each comprising three fundamental commands (refer to Table 1). For Path₁, there is one M (Move To) command and four Bézier curves. For Path₂, there is one M command and two line segments. To tokenize these paths, we first concatenate the commands of the two paths to form a single sequence. Then, we convert each command's 2D coordinates ($X = (x_0, y_0)$) into 1D using the formula $x_0 \times w + y$, where w is the bounding box size. We use a pretrained text encoder to tokenize the **text** "clock, time," where [CLS] and [SEP] mark the beginning and end of the text inputs. We then concatenate the embedded SVG and text sequences together and add a <SOS> at the beginning. This concatenated sequence is then sent to an autoregressive transformer to learn the joint probability distribution of the token sequences.

context. Some methods have been developed to increase the ability of autoregressive models to perform Fill-In-the-Middle (FIM) tasks by modifying training data without changing the model architecture. For example, CM3 [Aghajanyan et al. 2022] and InCoder [Fried et al. 2023] use a *causal masking* strategy that randomly selects several regions in the input sequence and moves them to the end. In [Bavarian et al. 2022], a similar strategy is implemented, and it is validated that this masking technique enables models to learn FIM without sacrificing their original generation capability. In our proposed method, we incorporate this technique so that our trained model can perform both left-to-right (autoregressive) generation and FIM tasks for SVG token sequences.

For a given input sequence S, we first select a random region called *span*, and split the sequence into three parts as [Left : Span : Right], where ":" represents concatenation. Then we replace the span with a special <Mask> token to obtain a new sequence S_1, i.e., $S_1 = $ [Left : <Mask> : Right]. Next, we add the same <Mask> token to the beginning of the span and add a <EOM> token (i.e., *end-of-mask*) to the end of the span to create a new sequence S_2, namely $S_2 = $ [<Mask> : Span : <EOM>]. Finally, we concatenate S_1 and S_2 to form the S' that we send to the model for training:

$$S' = [\text{Left} : \text{<Mask>} : \text{Right} : \text{<Mask>} : \text{Span} : \text{<EOM>}]. \quad (2)$$

The masked sequence S' conveys the following information: the first <Mask> token indicates the original position of the span, the second <Mask> token denotes the beginning of the span, and the <EOM> token marks the end of the span. During training, we randomly apply this masking strategy to 50% of the training data, while the remaining 50% do not have the special tokens <Mask> and <EOM>. We also exclude the <Mask> token from the calculation of the cross-entropy loss to ensure that the model does not generate it during inference.

We now explain how this masking technique can help an autoregressive model perform both left-to-right and FIM generation without modifying its architecture. For the left-to-right generation task, we do not need to pay extra attention because the model produces SVG tokens from left to right as usual, and this process will not produce any <Mask> tokens because we exclude them from the loss calculation. For the FIM task, suppose we have a sequence [Left : Right] and want to fill in the middle region between Left and Right. We add two <Mask> tokens to the sequence to create a new sequence [Left : <Mask> : Right : <Mask>], and send it to the model. The model then continues to generate tokens until the <EOM> token occurs, resulting in a sequence [Left : <Mask> : Right : <Mask> : Span : <EOM>]. Afterward, we move the Span to

its original position, i.e., the position of the first `<Mask>` token, to obtain the final output [`Left : Span : Right`]. Since the model uses both `Left` and `Right` information to complete the sequence, the `Span` is generated by considering bidirectional information, which is a form of "infilling".

3.4 Model Architecture

We employ the transformer architecture to implement our autoregressive model, as it can effectively capture the long-range interdependencies among the various tokens that constitute a vector icon sequence. The model consists of three modules: an SVG embedding module to encode the SVG sequence, a text embedding module to encode the text sequence, and a transformer module to exploit text-SVG correlations and learn the joint probability distribution of the token sequences. This allows the model to generate novel sequences that were not present in the training icon dataset.

SVG Embedding Module. As discussed in the previous two subsections, an SVG sequence is represented by six categories of distinct tokens: 1) 1D coordinates; 2) Command type; 3) Begin-of-path tokens `<BOP>`; 4) End-of-SVG tokens `<EOS>`; 5) Mask tokens `<Mask>` and 6) End-of-mask tokens `<EOM>`. Each icon has a 100×100 bounding box, resulting in 100^2 possible 1D coordinates. To represent different types of tokens, we convert them into one-hot vectors with a dimension of $10007 (= 100^2 + 3 + 1 + 1 + 1 + 1)$. We then use a learnable embedding matrix $\mathbf{W} \in \mathbb{R}^{d_{\text{model}} \times 10007}$ to transform one-hot vectors into d_{model}-sized vectors. We incorporate two extra learnable matrices $\mathbf{W}^x, \mathbf{W}^y \in \mathbb{R}^{d_{\text{model}} \times 100}$ to augment the coordinate information as in Xu et al. [2022]. The embedding of the i-th token is noted as:

$$e_i \leftarrow \mathbf{W}h_i + \mathbf{W}^x h_i^x + \mathbf{W}^y h_i^y + \mathbf{PE}_i, \tag{3}$$

where $h_i \in \mathbb{R}^{10007}$ is the one-hot vector of the i-th token. (h_i^x, h_i^y), where $h_i^x, h_i^y \in \mathbb{R}^{100}$, is the 2D coordinate of its 1D counterpart. We then add positional encoding $\mathbf{PE}_i$ to get the final embedding e_i.

Text Embedding Module. LLMs trained on a wide range of textual data have the ability to capture intricate word interrelationships, including synonymy and antonymy, as suggested in Saharia et al. [2022]. To harness the extensive knowledge embedded in LLMs, we extract the word embedding layer from a pretrained BERT [Turc et al. 2019] model and keep it fixed to handle textual inputs in our approach. We also use BERT's corresponding word tokenizer to discretize text descriptions. The tokenizer adds a [`CLS`] token to the beginning of the text and appends a [`SEP`] token at the end of the text, indicating the start and end of the text sequence, respectively.

Transformer Module. Our autoregressive transformer model consists of a stack of 12 identical layers. Each layer is a standard transformer decoder block comprising layer normalization, masked multi-head attention, multi-head attention, and feed-forward layers, all interconnected via residual connections. The autoregressive transformer ultimately produces a vector of dimension d_{model} at any given position n, which is conditioned on its preceding $n - 1$ tokens. To obtain the probability of all tokens occurring at position n, we employ a linear transformation and the softmax function.
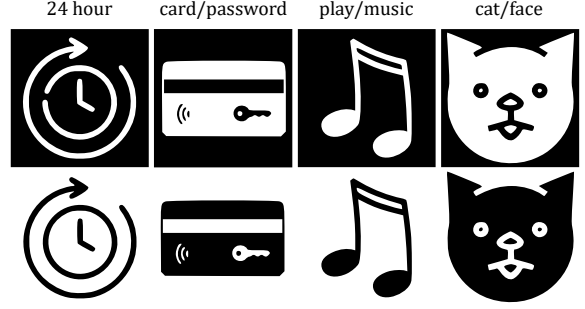

Fig. 3. Monochromatic icon samples from the *FIGR-8-SVG* dataset (1st row). Each icon is associated with several discrete words as class labels. We remove the black box to improve their visual quality (2nd row).

3.5 Training Objective

Our training objective is to regress both text and SVG sequences. Since the text descriptions and SVG scripts of different samples in the dataset have varying lengths, we pad both the text tokens $s_{\text{text}}^{\text{gt}}$ and SVG tokens $s_{\text{icon}}^{\text{gt}}$ converted from samples with zeros to a fixed size (512 for SVG tokens and 50 for text in our implementation). Once padded, we concatenate them to obtain the target sequence $s^{\text{gt}} = [s_{\text{text}}^{\text{gt}} : s_{\text{icon}}^{\text{gt}}]$.

The autoregressive transformer is trained to predict the next token based on previous tokens. To prepare the input sequence s^{in}, we remove the last token of s^{gt} (i.e., `<EOS>`) and add a `<SOS>` token at the start of s^{gt}. This operation shifts s^{gt} to the right by one position, resulting in the input sequence fed into the autoregressive transformer. The transformer outputs a token sequence $s^{\text{out}} = [s_{\text{text}}^{\text{out}} : s_{\text{icon}}^{\text{out}}]$ in a sequential manner, and our objective is to minimize the individual cross-entropy loss between the output and target tokens at each position, and then combine these losses by taking a weighted sum [Ramesh et al. 2021], as shown in the following equations:

$$\ell^{\text{text}} = \text{CE}(s_{\text{text}}^{\text{out}}, s_{\text{text}}^{\text{gt}}),$$
$$\ell^{\text{icon}} = \text{CE}(s_{\text{icon}}^{\text{out}}, s_{\text{icon}}^{\text{gt}}), \tag{4}$$
$$\ell^{\text{total}} = \lambda_t \ell^{\text{text}} + \lambda_i \ell^{\text{icon}},$$

where CE() is the standard cross-entropy function, $\lambda_t = 1.0$ and $\lambda_i = 7.0$ are the weighting terms controlling the relative importance between the text and icon reconstruction.

4 EXPERIMENTS

In this section, we first elaborate on the data processing procedure for the icon dataset and text input (Section 4.1). Then we introduce an ablation study to validate the efficacy of the model architecture under tasks of both conditional and unconditional generation settings (Section 4.2). Lastly, we compare the vector icons generated by our proposed framework with those from alternative solutions, demonstrating that our approach yields higher-quality results (Section 4.3).

4.1 Data Preparation

SVG Dataset. We use the *FIGR-8-SVG* dataset [Clouâtre and Demers 2019] that consists of 1.5 million monochromatic (black-and-white)

vector icons. Usually, the first step for SVG data processing is transforming icons with varied grammar into standardized representations. Fortunately, in the *FIGR-8-SVG* dataset, all icons have been converted to a uniform representation with discretized arguments. We show several icon examples from the dataset in the first row of Figure 3. We further enhance the visual attractiveness of each icon by removing the outer black box. The corresponding transformed icons are shown in the second row. After the SVG tokenization procedure detailed in Section 3.2, we set the maximum sequence length for an icon to 512, filtering out icons with exceeding sequence lengths and resulting in about 1.1 million samples. To boost efficiency, we select 300,000 samples for model training and experimentation. We partition these samples into 90% for training, 5% for validation, and 5% for testing.

Text Input. In the *FIGR-8-SVG* dataset, every vector icon is annotated with discrete keywords as class labels, such as "`cat/face`". Training the model only with keywords would constrain our model's capacity to generate icons from natural language sentences. Inspired by InstructPix2Pix [Brooks et al. 2022], which fine-tunes GPT-3 [Brown et al. 2020] to produce edit instructions and captions, we use LLMs (ChatGPT* in particular) to convert these keywords into natural language phrases and sentences. The prompt given to ChatGPT is "`Write the simplest sentence from keywords: #{keywords}. Do not add additional facts`". However, it is crucial to recognize the potential risk of unintended mismatches between text and SVG when sentences are generated from keywords without human oversight.

Implementation Details. We implement the framework using *PyTorch*. The training process employs the Adam optimizer [Kingma and Ba 2014] with a learning rate of 0.0006, along with linear warm-up and decay. The dropout rate is set to 0.1, and we also use gradient clipping. Text descriptions containing shuffled discrete labels, natural language sequences generated by ChatGPT, and blank text are respectively trained with probabilities of 60%, 30%, and 10%, with a total batch size of 192 and 300 epochs. We use an NVIDIA A100 GPU in the following experiments to test our model. It takes 1.38 seconds to generate an SVG icon sequence on average.

Metrics. To evaluate the quality of the generated SVG icons, we use the Fréchet Inception Distance (FID) [Heusel et al. 2017] by measuring the distance between the image features of synthetic and real SVG icons. Specifically, we obtain the image features of rendered SVG icons using the CLIP image encoder [Radford et al. 2021]. We also compute the CLIP score to measure text-SVG alignment (i.e., the semantic similarity between the text input and the visual icon output). Additionally, following SkexGen [Xu et al. 2022], we calculate the "Novelty" and the "Uniqueness" scores in our quantitative evaluation. The "Novelty" score refers to the proportion of generated data absent from the target set, and the "Uniqueness" score denotes the percentage of data that occurs solely once within the generated samples (in calculation, we sample 20,000 icons for random generation and 7,000 icons for text-guided generation). When computing these two scores, we use the cosine similarity between CLIP features to determine whether the two icons are identical. We

---

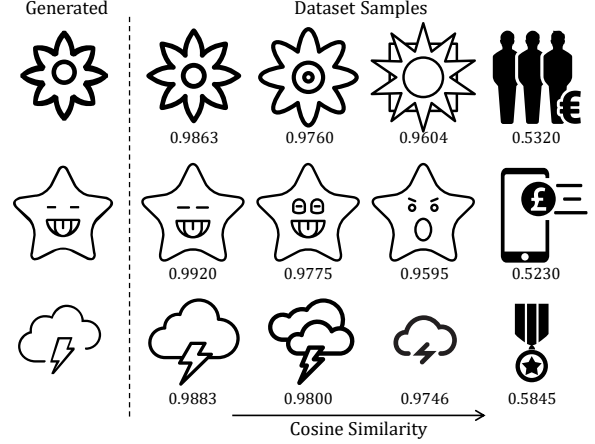*https://openai.com/blog/chatgpt

Fig. 4. We use the CLIP image encoder to extract image features and calculate the cosine similarity between the generated icons and the samples in the dataset. However, visually distinct icons may have high cosine similarity scores due to the simple strokes and white backgrounds of monochromatic icons. Therefore, we selected a high threshold of **0.98** to determine whether two icons are identical when computing the "Uniqueness" and "Novelty" scores.

set the threshold to **0.98** in experiments. Figure 4 gives an intuitive visual comparison of the similarity values.

4.2 Ablation on Different Network Architecture

In this subsection, we conduct two ablation studies to illustrate the effects of two key components of our proposed method. The first study shows the importance of preserving the sequential nature of the SVG icons in generation by comparing our seq2seq model to a GAN model. The second study demonstrates the necessity of our autoregressive model augmented with a masking scheme by comparing two seq2seq transformer training strategies: our autoregressive model versus a non-autoregressive model (i.e., BERT [Devlin et al. 2018]).

Seq2seq versus GAN. As previously mentioned, an SVG file is structured hierarchically, consisting of high-level paths and low-level commands. Here we use DeepSVG+GAN as a baseline to testify our choice of sequence-preserving generation mechanism.

The original DeepSVG reconstructs an SVG icon by first obtaining a vector representation of each low-level element, which is then averaged to generate a global representation z. To conduct a fair comparison between our method and DeepSVG, we need to enable the original DeepSVG framework to generate new icons and support text-conditioned generation. To achieve these goals, we first train an AutoEncoder, as introduced in DeepSVG, for SVG icon reconstruction on our dataset. We then train a conditional GAN model with text features as input to obtain the latent vector z, which can be decoded into an SVG icon after passing through the decoder of the AutoEncoder. In addition to text-driven generation, we also enable the GAN to generate icons independently without textual descriptions by replacing the text feature with random noise 10% of the time.

We thus compare the generation performance regarding both *Random Generation* and *Text-Guided Generation* tasks. For random
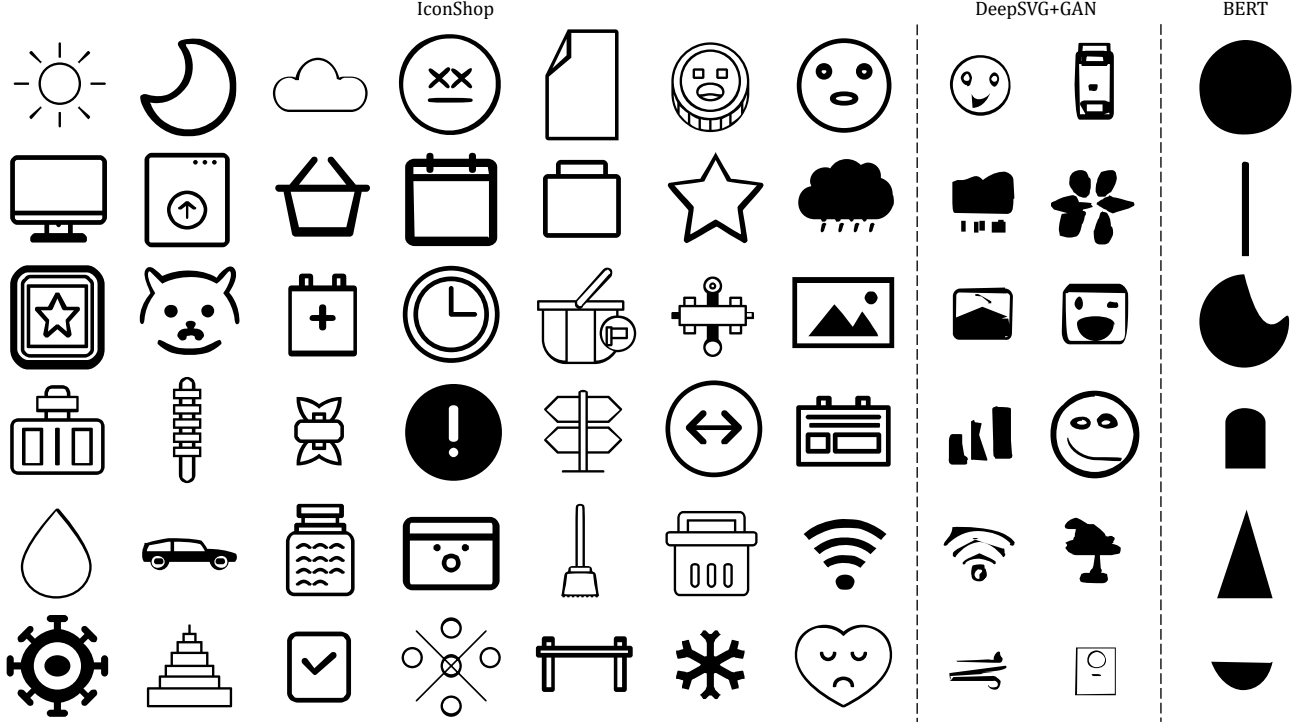
IconShop DeepSVG+GAN BERT

Fig. 5. Icons randomly generated by IconShop, DeepSVG+GAN and BERT. Our approach creates icons that maintain geometric relationships, such as perpendicularity and parallelism. Icons produced by DeepSVG+GAN do not meet the desired quality, while BERT only synthesizes basic geometric shapes.

generation, we produce 20,000 icons for each method. For text-guided generation, we chose both discrete keywords and natural phrases/sentences commonly used in design scenarios as text input and collected 7,000 generated icons for both models. As shown in Figures 5 and 6, our approach is capable of generating visually pleasing icons while preserving complex geometric relationships, such as perpendicularity, parallelism and symmetry, as we prioritize the sequential property of SVG icons throughout the entire generation process. In contrast, DeepSVG+GAN fails to produce icons with the above-mentioned properties and presents relatively worse results than ours. We attribute DeepSVG's deficient performance to its averaging operation over commands and paths, resulting in a loss of details in the generated icons. Please refer to the project page for more qualitative results.

We also quantitatively evaluate the results generated by these two methods. Details of the comparisons in random generation and text-guided generation tasks can be found in Tables 2a and 2b, respectively. It shows that IconShop can synthesize results with significantly lower FID values in both random and text-guided generation tasks, indicating our approach's superior generation performance. Regarding the Uniqueness and Novelty metrics, our system performs comparably well to DeepSVG+GAN, highlighting the rich diversity in our results. However, it is important to note that the high Uniqueness and Novelty values exhibited by DeepSVG+GAN are primarily a result of the noticeable jittering curves it creates, as evident in Figure 5. We regard this phenomenon as "fake diversity". Moreover, our method has the highest CLIP score in the text-guided generation task, signaling our outstanding ability to produce icons that accurately reflect the semantic context of the text input.

	FID ↓	Uniqueness% ↑	Novelty% ↑
DeepSVG+GAN	11.95	**98.72**	**99.22**
BERT	43.61	2.06	19.90
IconShop	**6.08**	78.77	85.10

(a) Random Generation

	FID ↓	Uniqueness% ↑	Novelty% ↑	CLIP Score ↑
DeepSVG+GAN	12.01	**97.59**	**99.01**	21.78
BERT	35.10	14.41	50.30	22.03
IconShop	**4.65**	68.29	68.60	**25.74**

(b) Text-Guided Generation

Table 2. We evaluated our approach through random generation and text-guided generation tasks. We used the FID score, with features extracted from the CLIP image encoder, to assess generation quality. We also computed the percentage of unique and novel icons to show their diversity. For text-guided generation, we used the CLIP score to show the alignment between the text input and the generated icons.

AR versus BERT. Recent research [Chang et al. 2023, 2022] suggests that using a non-autoregressive training paradigm for generating rasterized images is feasible. These approaches use bidirectional Transformers (i.e., BERT) as the fundamental model architecture. The alteration from the autoregressive model to BERT allows for the simultaneous prediction of multiple masked tokens and enables the model to undertake diverse image editing tasks such as inpainting. A plausible proposal is to explore the possibility of using the BERT model to produce SVG token sequences with its fast inference speed and "zero-shot" FIM capabilities, as an alternative to our masking scheme introduced in Section 3.3. However, there exists a notable distinction between raster image tokenization and icon sequence tokenization: The former resizes the input images to the same shape
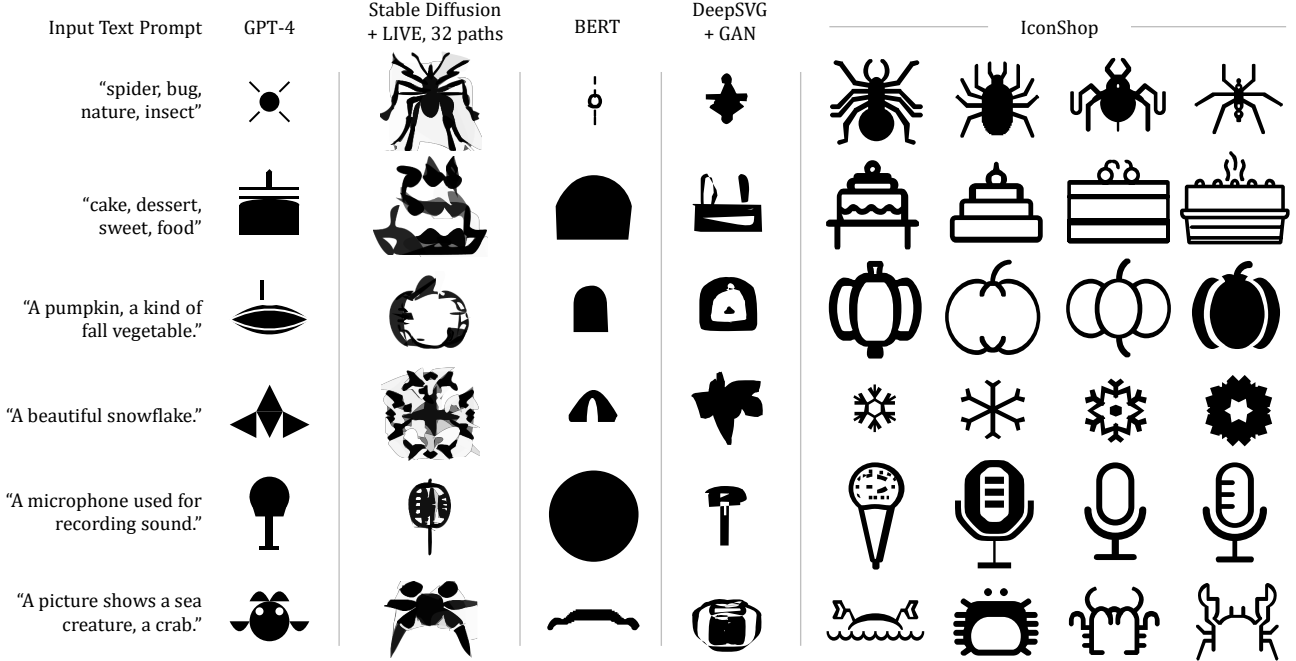
Fig. 6. We evaluate the text-guided icon synthesis of IconShop against several other methods, including the language-based method (GPT-4), image-based method (Stable Diffusion+LIVE), BERT, and DeepSVG+GAN. The results show that GPT-4 only produces combinations of basic geometric shapes, while Stable Diffusion+LIVE has poor vectorization results. Our IconShop outperforms other frameworks in terms of icon generation quality.

and generates outputs of fixed length, whereas the latter produces outputs of varying length. Thus the training complexities of these two cases are different, because the BERT model adopted in our task needs to not only consider the likelihood of tokens appearing at different positions but also determine where to terminate the sequence. After training the BERT model with the same dataset as ours, we assess the quality of its outputs.

Quantitative evaluations are conducted similarly to DeepSVG+GAN in both random (Table 2a) and text-guided generation (Table 2b). BERT produces results with relatively worse quality in both tasks, showing inferior quality to ours and DeepSVG+GAN. The qualitative results in Figure 5 suggest that BERT can only generate simple geometric shapes such as circles and rectangles. Our observations reveal that during inference, the end-of-SVG token <EOS> frequently appears in multiple positions, resulting in early termination when reconstructing SVG icons from token sequences. Therefore, we hold the perspective that despite the BERT model's impressive ability in sequence editing, it is inferior to our approach in generating sequences of varying lengths.

4.3 Comparison to State-of-the-Art Approaches

As previously mentioned, there are two types of text-to-SVG generation frameworks: image-based and language-based methods. For the language-based approach, we employ GPT-4, a powerful pretrained large language model, to generate SVG text scripts directly. To initiate the conversation, we provide an additional prompt asking it to act as an SVG code generator. For the image-based approach, we use Stable Diffusion [Rombach et al. 2022] to create rasterized images, which we then transform into SVG format using the Layer-wise Image VEctorization (LIVE) [Ma et al. 2022] program. To produce

vectorized results in our desired icon styles, we include extra keywords (like "monochrome" and "line art") in the text descriptions during the generation process.

Figure 6 shows icons synthesized by various frameworks. We can see that GPT-4 has relatively strong capabilities in generating SVG scripts for 2D icons from text prompts, with moderate text-SVG alignment. Nevertheless, the results are simple combinations of primitive shapes with no complex overlapping or penetration, which is inadequate for graphics usage. With respect to image-based methods, the outcomes often fall short of expectations because the Stable Diffusion model, which is trained on raster images, struggles to produce icon-style images even with some prompt engineering. After applying the LIVE, the resulting SVG icons usually present unsmooth paths with sharp corners, crossovers and messy structural relations (i.e., perpendicularity and parallelism). This method is also rather inefficient, as the LIVE is optimization-based and hence time-consuming, rendering it unsuitable for real-time applications. Compared to the competing methods, our IconShop produces results with the highest visual quality and text alignment, demonstrating exceptional generation capabilities in the text-to-icon task. More visual results of the text-guided generation can be found in our project page.

4.4 User Study

To further evaluate the visual quality of vector icons produced by different methods, we conducted a perceptive user study consisting of three tasks: (1) In the first task, we calculate the fooling rates of high-quality icons for different methods. Before starting the study, we present users with icons from the training dataset to set a standard for high quality. We then mix 15 icons randomly generated
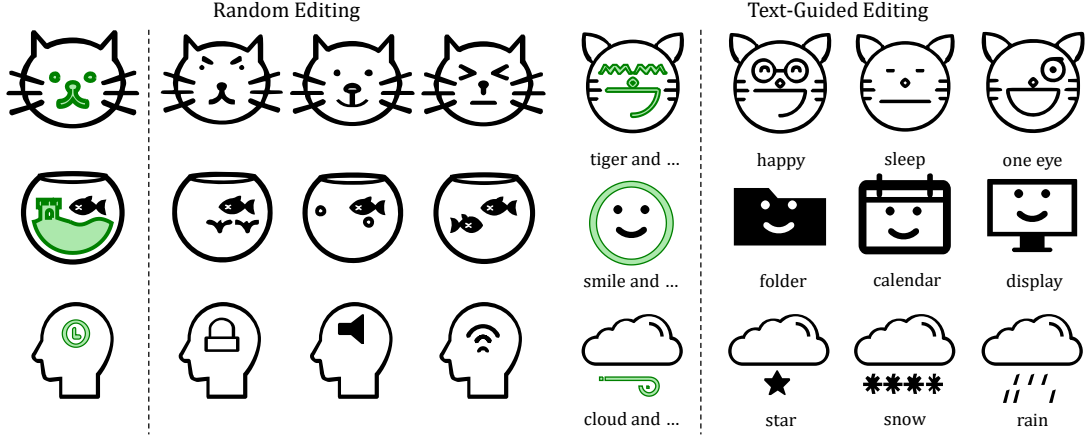
Fig. 7. Our proposed method can achieve both random and text-guided icon editing, enabling users to edit paths in icons. We use green color to highlight the paths to be edited.

by each of the four frameworks (IconShop, DeepSVG+GAN, Stable Diffusion+LIVE, and GPT-4) with 15 icons from our dataset, resulting in a total of 75 icons. Users are asked to give a binary choice of whether the individual icon is of high-quality in this mix. (2) In the second task, we randomly select ten text prompts and generate corresponding icons from each framework. Users are then asked to select the top two icons they believe are of the best visual quality. (3) The third task also involves ten text prompts and icon generation, but this time, users need to pick the top two icons that best semantically align with the text prompt.

We conducted the user study via an online questionnaire, with 79 users participating in the study. For the first task, we obtained 79 (users) × 15 (icons) × 5 (methods) = 5925 subjective judgments. We calculated the averaged percentage of users identifying icons as high-quality for each method, and the results are shown in the first row of Table 3. We can see that our method has a similar performance to the "Dataset" and is superior to the other three methods, indicating that the quality of the unconditional (random) generated results is of similar quality to the dataset.

For tasks two and three, we collected 79 (users) × 10 (cases) × 2 (selections) = 1580 subjective judgments for each task. We report the user selection proportions in rows 2 and 3 of Table 3, respectively. It demonstrates that our model's synthesized icons are most frequently selected, indicating the highest quality and the best text-SVG alignment in the text-guided generation task. We also performed a one-way ANOVA test on the averaged user selection proportions over each input. Both p-values were less than 0.001, suggesting statistically significant differences in the methods' performance across tasks. Overall, our IconShop demonstrates the highest quality for both random and text-guided generation, with a strong alignment between the input text and synthesized SVG.

5 APPLICATION

Our proposed framework enables four practical icon applications: icon editing, icon interpolation, semantic combination of icons, and auto-suggestion for icon design. These applications streamline the process of vector icon creation, enhancing user productivity and experience significantly.

	User Selection% ↑				
	GPT-4	Stable Diffusion + LIVE	DeepSVG + GAN	IconShop	Dataset
Quality (random)	54.09	15.95	2.95	82.11	**83.71**
Quality (text)	51.90	49.49	2.15	**96.33**	\
Align (text)	29.24	72.78	1.77	**96.20**	\

Table 3. User study results. In the first row (task 1), we report the average percentage of users identifying randomly generated icons as high-quality for each method. In the second row (task 2), we report the average user selection proportions of each method for the best quality in text-guided icon generation, and in the third row (task 3), we report the average user selection proportions of each method for the best text-SVG alignment in text-guided icon generation.

5.1 Icon Editing

Conventional autoregressive models, due to their unidirectional token generation, are ill-suited for editing tasks. Nonetheless, the masking scheme, as outlined in Section 3.3, effectively addresses this limitation, facilitating icon editing as exemplified in Figure 7. Our model can fill in missing contents based on bidirectional information, irrespective of whether it is text-guided. This leads to precise, consistent, and diverse predictions for restoring the missing paths in icons.

5.2 Icon Interpolation

In the DeepSVG framework, each SVG icon is encoded to obtain a latent vector z, allowing for convenient manipulation of the latent space by interpolating latent vectors. However, in IconShop, we convert each icon to a uniquely decodable token sequence, making direct interpolation infeasible. Instead, our model support interpolating the text embedding vectors and generating icons for each interpolated vector. Figure 8 shows a collection of icons generated from interpolated text embedding vectors, demonstrating that our model has learned a smooth mapping function between the text and SVG spaces.

5.3 Semantic Combination of Icons

Text-to-image models demonstrate an impressive ability to combine textual inputs, allowing them to generate novel concepts that do
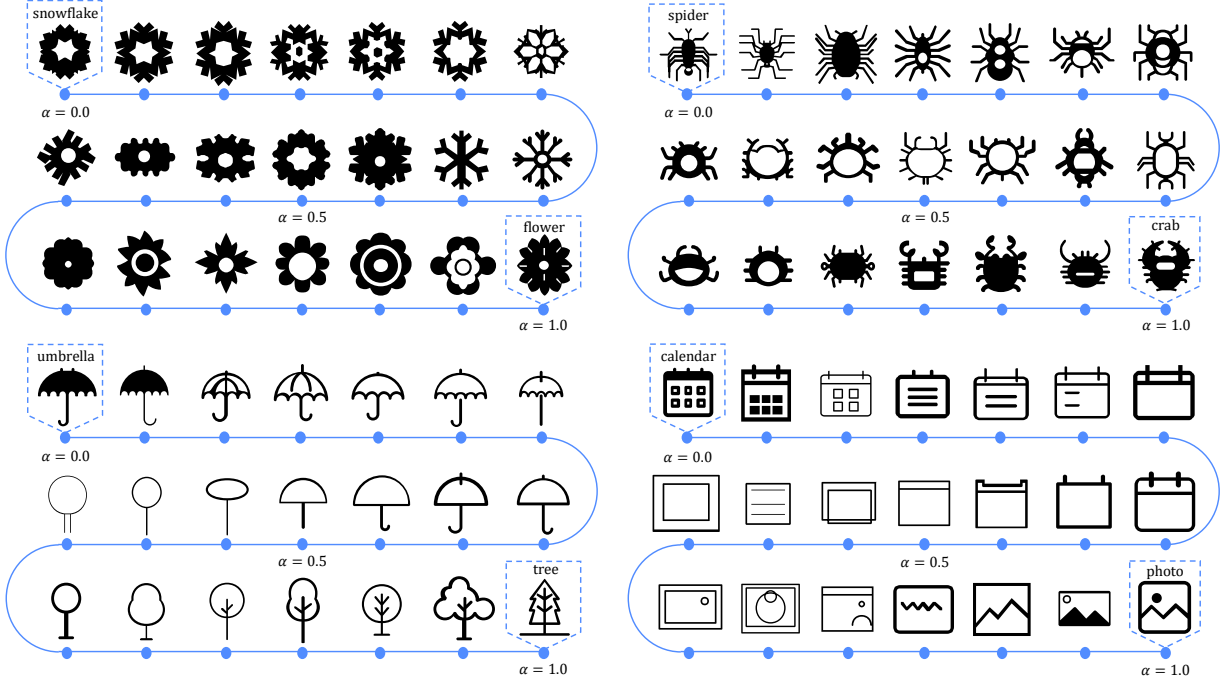
Fig. 8. We interpolate text embedding vectors using the formula $v' = (1 - \alpha) \cdot v_1 + \alpha \cdot v_2$, where v_1 and v_2 represent text embedding vectors and $\alpha \in [0, 1]$. Subsequently, we generate icons corresponding to each interpolated vector v'. The results show that our model learns a smooth mapping function between the text and SVG spaces.

not exist in the training data, such as "avocado chair" generated by DALL·E [Ramesh et al. 2021]. In our experiments, we find that our model can also produce innovative and creative combinations, as shown in Figure 9.
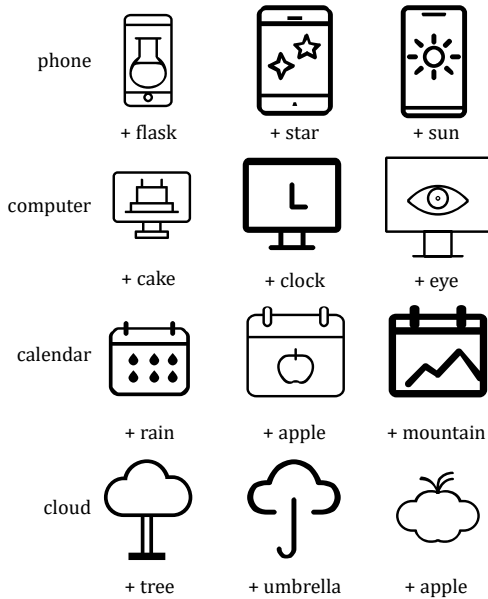
5.4 Auto-Suggestion for Icon Design

One advantage of automatic icon generation is to develop a computational framework that can support both designers and non-specialists in expressing their creative ideas. A desired feature of such a system is the ability to suggest possible placements for subsequent paths on a canvas, which can significantly improve workflow efficiency and productivity. By leveraging autoregressive transformers and preserving the sequential characteristics of SVG icons, our trained model can predict the next path that users may need to

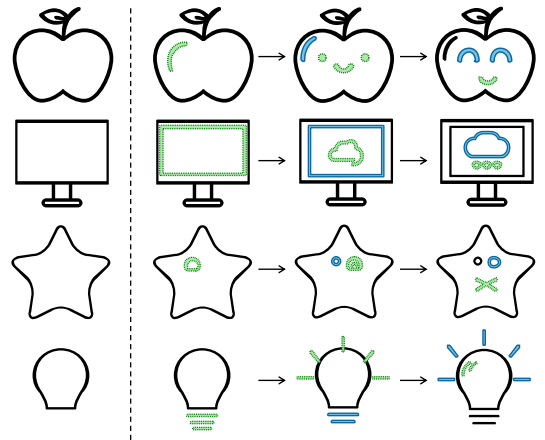Fig. 9. Our model can produce creative icons by semantic combination.

Fig. 10. Our model can suggest subsequent paths for designers to draw icons, notably boosting creation efficiency. We highlight paths suggested by the model with green colors and paths drawn by users with blue colors. Even if users diverge from the suggested route, our model can still predict subsequent paths based on previous icon sequences.
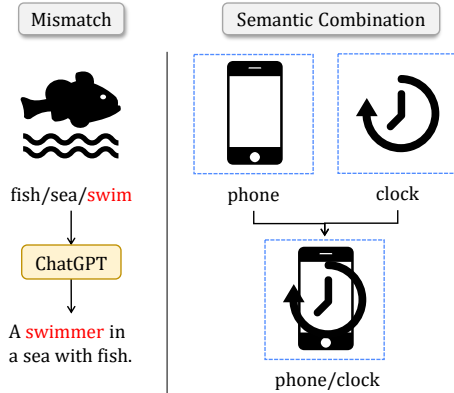
Fig. 11. Limitations contain text-SVG mismatches (left) and suboptimal semantic combination performance (right).

implement in their icon creation process (Figure 10). Please refer to our project page to watch videos demonstrating the interactive auto-suggestion system for icon design.

6 CONCLUSION

In this paper, we introduce IconShop, an autoregressive transformer-based method proficient at generating vector icons from textual descriptions. Our approach stands out from both image-based methods that combine text-to-image generation and image vectorization methods, and language-based techniques that treat SVG scripts as languages. Instead, we sequentialize and tokenize the SVG paths into a uniquely decodable command sequence that facilitates seamless end-to-end model training. Comprehensive experiments showcase the effectiveness and robustness of our model in terms of generation quality, diversity and accurate text-icon alignment. Furthermore, multiple icon synthesis applications supported by IconShop indicate its flexibility in practical use cases.

Limitations. Although IconShop exhibits impressive performance with respect to the generation quality and diversity, our methods have certain limitations (Figure 11). Firstly, natural language phrases and sentences generated by ChatGPT may inadvertently result in text-SVG mismatches. This problem can be mitigated by using a high-quality SVG dataset with accurate text annotation or by implementing human filtering. Secondly, the model's semantic combination performance may not be as remarkable as text-to-image generation, because most icons in the *FIGT-8-SVG* dataset contain a single object situated at the center, occupying a significant portion of the space. However, proper data augmentation techniques such as scaling and merging the data to create new icons could notably improve the combination performance. Finally, our IconShop could potentially be expanded to yield more complex outputs like multicolored icons and clip art with proper modifications. Exploring these promising avenues remains a task for future endeavors.

REFERENCES

Armen Aghajanyan, Bernie Huang, Candace Ross, Vladimir Karpukhin, Hu Xu, Naman Goyal, Dmytro Okhonko, Mandar Joshi, Gargi Ghosh, Mike Lewis, and Luke Zettlemoyer. 2022. CM3: A Causal Masked Multimodal Model of the Internet. *arXiv preprint arXiv:2201.07520*.

Haruka Aoki and Kiyoharu Aizawa. 2022. SVG Vector Font Generation for Chinese Characters with Transformer. In *IEEE International Conference on Image Processing*. 646–650.

Mohammad Bavarian, Heewoo Jun, Nikolas Tezak, John Schulman, Christine McLeavey, Jerry Tworek, and Mark Chen. 2022. Efficient Training of Language Models to Fill in the Middle. *arXiv preprint arXiv:2207.14255*.

Steven Bergen and Brian J. Ross. 2012. Automatic and Interactive Evolution of Vector Graphics Images with Genetic Algorithms. *The Visual Computer* 28, 1, 35–45.

Tim Brooks, Aleksander Holynski, and Alexei A. Efros. 2022. InstructPix2Pix: Learning to Follow Image Editing Instructions. *arXiv preprint arXiv:2211.09800*.

Tom B. Brown, Benjamin Mann, Nick Ryder, Melanie Subbiah, Jared Kaplan, Prafulla Dhariwal, Arvind Neelakantan, Pranav Shyam, Girish Sastry, Amanda Askell, Sandhini Agarwal, Ariel Herbert-Voss, Gretchen Krueger, Tom Henighan, Rewon Child, Aditya Ramesh, Daniel M. Ziegler, Jeffrey Wu, Clemens Winter, Christopher Hesse, Mark Chen, Eric Sigler, Mateusz Litwin, Scott Gray, Benjamin Chess, Jack Clark, Christopher Berner, Sam McCandlish, Alec Radford, Ilya Sutskever, and Dario Amodei. 2020. Language Models are Few-Shot Learners. In *Advances in Neural Information Processing Systems*. 1877–1901.

Sébastien Bubeck, Varun Chandrasekaran, Ronen Eldan, Johannes Gehrke, Eric Horvitz, Ece Kamar, Peter Lee, Yin-Tat Lee, Yuanzhi Lee, Scott Lundberg, Harsha Nori, Hamid Palangi, Macro T. Ribeiro, and Yi Zhang. 2023. Sparks of Artificial General Intelligence: Early Experiments with GPT-4. *arXiv preprint arXiv:2303.12712*.

Alexandre Carlier, Martin Danelljan, Alexandre Alahi, and Radu Timofte. 2020. DeepSVG: A Hierarchical Generative Network for Vector Graphics Animation. In *Advances in Neural Information Processing Systems*. 16351–16361.

Huiwen Chang, Han Zhang, Jarred Barber, Aaron Maschinot, Jose Lezama, Lu Jiang, Ming-Hsuan Yang, Kevin Murphy, William T. Freeman, Michael Rubinstein, Yuanzhen Li, and Dilip Krishnan. 2023. Muse: Text-To-Image Generation via Masked Generative Transformers. *arXiv preprint arXiv:2301.00704*.

Huiwen Chang, Han Zhang, Lu Jiang, Ce Liu, and William T. Freeman. 2022. MaskGIT: Masked Generative Image Transformer. In *IEEE Conference on Computer Vision and Pattern Recognition*. 11315–11325.

Mark Chen, Alec Radford, Rewon Child, Jeffrey Wu, Heewoo Jun, David Luan, and Ilya Sutskever. 2020. Generative Pretraining from Pixels. In *International Conference on Machine Learning*. 1691–1703.

Louis Clouâtre and Marc Demers. 2019. FIGR: Few-shot Image Generation with Reptile. *arXiv preprint arXiv:1901.02199*.

Jacob Devlin, Ming-Wei Chang, Kenton Lee, and Kristina Toutanova. 2018. BERT: Pre-training of Deep Bidirectional Transformers for Language Understanding. *arXiv preprint arXiv:1810.04805*.

Ming Ding, Zhuoyi Yang, Wenyi Hong, Wendi Zheng, Chang Zhou, Da Yin, Junyang Lin, Xu Zou, Zhou Shao, Hongxia Yang, and Jie Tang. 2021. CogView: Mastering Text-to-Image Generation via Transformers. In *Advances in Neural Information Processing Systems*. 19822–19835.

Ming Ding, Wendi Zheng, Wenyi Hong, and Jie Tang. 2022. CogView2: Faster and Better Text-to-Image Generation via Hierarchical Transformers. *arXiv preprint arXiv:2204.14217*.

Patrick Esser, Robin Rombach, and Bjorn Ommer. 2021. Taming Transformers for High-Resolution Image Synthesis. In *IEEE Conference on Computer Vision and Pattern Recognition*. 12873–12883.

Kevin Frans, Lisa B. Soros, and Olaf Witkowski. 2021. CLIPDraw: Exploring Text-to-Drawing Synthesis through Language-Image Encoders. *arXiv preprint arXiv:2106.14843*.

Daniel Fried, Armen Aghajanyan, Jessy Lin, Sida Wang, Eric Wallace, Freda Shi, Ruiqi Zhong, Wen-tau Yih, Luke Zettlemoyer, and Mike Lewis. 2023. InCoder: A Generative Model for Code Infilling and Synthesis. In *International Conference on Learning Representations*.

Ian Goodfellow, Jean Pouget-Abadie, Mehdi Mirza, Bing Xu, David Warde-Farley, Sherjil Ozair, Aaron Courville, and Yoshua Bengio. 2014. Generative Adversarial Nets. In *Advances in Neural Information Processing Systems*. 2672–2680.

David Ha and Douglas Eck. 2017. A Neural Representation of Sketch Drawings. *arXiv preprint arXiv:1704.03477*.

Martin Heusel, Hubert Ramsauer, Thomas Unterthiner, Bernhard Nessler, and Sepp Hochreiter. 2017. GANs Trained by a Two Time-Scale Update Rule Converge to a Local Nash Equilibrium. In *Advances in Neural Information Processing Systems*. 6629–6640.

Jonathan Ho, Ajay Jain, and Pieter Abbeel. 2020. Denoising Diffusion Probabilistic Models. In *Advances in Neural Information Processing Systems*. 6840–6851.

Cheng-Zhi Anna Huang, Ashish Vaswani, Jakob Uszkoreit, Noam Shazeer, Ian Simon, Curtis Hawthorne, Andrew M. Dai, Matthew D. Hoffman, Monica Dinculescu, and Douglas Eck. 2018. Music Transformer. *arXiv preprint arXiv:1809.04281*.

Ajay Jain, Amber Xie, and Pieter Abbeel. 2022. VectorFusion: Text-to-SVG by Abstracting Pixel-Based Diffusion Models. *arXiv preprint arXiv:2211.11319*.

Minguk Kang, Jun-Yan Zhu, Richard Zhang, Jaesik Park, Eli Shechtman, Sylvain Paris, and Taesung Park. 2023. Scaling up GANs for Text-to-Image Synthesis. *arXiv preprint arXiv:2303.05511*.

Diederik P. Kingma and Jimmy Ba. 2014. Adam: A Method for Stochastic Optimization. *arXiv preprint arXiv:1412.6980*.

Diederik P. Kingma and Max Welling. 2013. Auto-Encoding Variational Bayes. *arXiv preprint arXiv:1312.6114*.

Naihan Li, Shujie Liu, Yanqing Liu, Sheng Zhao, and Ming Liu. 2019. Neural Speech Synthesis with Transformer Network. In *AAAI Conference on Artificial Intelligence*. 6706–6713.

Tzu-Mao Li, Michal Lukáč, Gharbi Michaël, and Jonathan Ragan-Kelley. 2020. Differentiable Vector Graphics Rasterization for Editing and Learning. *ACM Transactions on Graphics* 39, 6, 193:1–193:15.

Raphael G. Lopes, David Ha, Douglas Eck, and Jonathon Shlens. 2019. A Learned Representation for Scalable Vector Graphics. In *IEEE International Conference on Computer Vision*. 7930–7939.

Xu Ma, Yuqian Zhou, Xingqian Xu, Bin Sun, Valerii Filev, Nikita Orlov, Yun Fu, and Humphrey Shi. 2022. Towards Layer-wise Image Vectorization. In *IEEE Conference on Computer Vision and Pattern Recognition*. 16314–16323.

Alex Nichol, Prafulla Dhariwal, Aditya Ramesh, Pranav Shyam, Pamela Mishkin, Bob McGrew, Ilya Sutskever, and Mark Chen. 2021. GLIDE: Towards Photorealistic Image Generation and Editing with Text-Guided Diffusion Models. *arXiv preprint arXiv:2112.10741*.

OpenAI. 2023. GPT-4 Technical Report. *arXiv preprint arXiv:2303.08774*.

Ben Poole, Ajay Jain, Jonathan T. Barron, and Ben Mildenhall. 2022. Dreamfusion: Text-to-3D using 2D Diffusion. *arXiv preprint arXiv:2209.14988*.

Steve Probets, Julius Mong, David Evans, and David Brailsford. 2001. Vector Graphics: From PostScript and Flash to SVG. In *ACM Symposium on Document Engineering*. 135–143.

Tingting Qiao, Jing Zhang, Duanqing Xu, and Dacheng Tao. 2019. MirrorGAN: Learning Text-to-image Generation by Redescription. In *IEEE Conference on Computer Vision and Pattern Recognition*. 1505–1514.

Alec Radford, Jong-Wook Kim, Chris Hallacy, Aditya Ramesh, Gabriel Goh, Sandhini Agarwal, Girish Sastry, Amanda Askell, Pamela Mishkin, Jack Clark, Gretchen Krueger, and Ilya Sutskever. 2021. Learning Transferable Visual Models From Natural Language Supervision. In *International Conference on Machine Learning*. 8748–8763.

Alec Radford, Jeffrey Wu, Rewon Child, David Luan, Dario Amodei, and Ilya Sutskever. 2019. Language Models are Unsupervised Multitask Learners. *OpenAI blog* 1, 8, 9.

Colin Raffel, Noam Shazeer, Adam Roberts, Katherine Lee, Sharan Narang, Michael Matena, Yanqi Zhou, Wei Li, and Peter J. Liu. 2020. Exploring the Limits of Transfer Learning with a Unified Text-to-Text Transformer. *The Journal of Machine Learning Research* 21, 1, 5485–5551.

Aditya Ramesh, Mikhail Pavlov, Gabriel Goh, Scott Gray, Chelsea Voss, Alec Radford, Mark Chen, and Ilya Sutskever. 2021. Zero-Shot Text-to-Image Generation. In *International Conference on Machine Learning*. 8821–8831.

Scott Reed, Zeynep Akata, Xinchen Yan, Lajanugen Logeswaran, Bernt Schiele, and Honglak Lee. 2016. Generative Adversarial Text to Image Synthesis. In *International Conference on Machine Learning*. 1060–1069.

Robin Rombach, Andreas Blattmann, Dominik Lorenz, Patrick Esser, and Björn Ommer. 2022. High-Resolution Image Synthesis with Latent Diffusion Models. In *IEEE Conference on Computer Vision and Pattern Recognition*. 10684–10695.

Chitwan Saharia, William Chan, Saurabh Saxena, Lala Li, Jay Whang, Emily Denton, Seyed K. S. Ghasemipour, Burcu-Karagol Ayan, S. Sara Mahdavi, Rapha G. Lopes, Tim Salimans, Jonathan Ho, David J. Fleet, and Mohammad Norouzi. 2022. Photorealistic Text-to-Image Diffusion Models with Deep Language Understanding. In *Advances in Neural Information Processing Systems*. 36479–36494.

Peter Selinger. 2003. Potrace: A polygon-based tracing algorithm.

Iulia Turc, Ming-Wei Chang, Kenton Lee, and Kristina Toutanova. 2019. Well-Read Students Learn Better: On the Importance of Pre-training Compact Models. *arXiv preprint arXiv:1908.08962v2*.

Rafael Valle, Kevin Shih, Ryan Prenger, and Bryan Catanzaro. 2020. Flowtron: An Autoregressive Flow-based Generative Network for Text-to-Speech Synthesis. *arXiv preprint arXiv:2005.05957*.

Ashish Vaswani, Noam Shazeer, Niki Parmar, Jakob Uszkoreit, Llion Jones, Aidan N. Gomez, Łukasz Kaiser, and Illia Polosukhin. 2017. Attention Is All You Need. In *Advances in Neural Information Processing Systems*. 6000–6010.

Tao Xu, Pengchuan Zhang, Qiuyuan Huang, Han Zhang, Zhe Gan, Xiaolei Huang, and Xiaodong He. 2018. AttnGAN: Fine-Grained Text to Image Generation with Attentional Generative Adversarial Networks. In *IEEE Conference on Computer Vision and Pattern Recognition*. 1316–1324.

Xiang Xu, Karl D. D. Willis, Joseph G. Lambourne, Chin-Yi Cheng, Pradeep K. Jayaraman, and Yasutaka Furukawa. 2022. SkexGen: Autoregressive Generation of CAD Construction Sequences with Disentangled Codebooks. In *International Conference on Machine Learning*. 24698–24724.

Jiahui Yu, Yuanzhong Xu, Jing-Yu Koh, Thang Luong, Gunjan Baid, Zirui Wang, Vijay Vasudevan, Alexander Ku, Yinfei Yang, Burcu-Karagol Ayan, Ben Hutchinson, Wei Han, Zarana Parekh, Xin Li, Han Zhang, Jason Baldridge, and Yonghui Wu. 2022. Scaling Autoregressive Models for Content-Rich Text-to-Image Generation. *arXiv preprint arXiv:2206.10789*.

Han Zhang, Tao Xu, Hongsheng Li, Shaoting Zhang, Xiaogang Wang, Xiaolei Huang, and Dimitris N. Metaxas. 2017. StackGAN: Text to Photo-realistic Image Synthesis with Stacked Generative Adversarial Networks. In *IEEE International Conference on Computer Vision*. 5907–5915.

Zhu Zhang, Jianxin Ma, Chang Zhou, Rui Men, Zhikang Li, Ming Ding, Jie Tang, Jingren Zhou, and Hongxia Yang. 2021. M6-UFC: Unifying Multi-Modal Controls for Conditional Image Synthesis via Non-Autoregressive Generative Transformers. *arXiv preprint arXiv:2105.14211*.

Zizhao Zhang, Yuanpu Xie, and Lin Yang. 2018. Photographic Text-to-Image Synthesis with a Hierarchically-nested Adversarial Network. In *IEEE Conference on Computer Vision and Pattern Recognition*. 6199–6208.